QED calculation of two-electron one-photon transition probabilities in He-like ions

Konstantin N. Lyashchenko *
Institute of Modern Physics, Chinese Academy of Sciences, Lanzhou 730000, China

Oleg Yu. Andreev
Department of Physics, St. Petersburg State University, 7/9 Universitetskaya nab., St. Petersburg 199034, Russia and Petersburg Nuclear Physics Institute named by B.P. Konstantinov of National Research Centre "Kurchatov Institute", Gatchina, Leningrad District 188300, Russia

Deyang Yu
Institute of Modern Physics, Chinese Academy of Sciences, Lanzhou 730000, China and University of Chinese Academy of Sciences, Beijing 100049, China

(Received 27 April 2021; revised 8 July 2021; accepted 13 July 2021; published 29 July 2021)

We consider theoretically the process of two-electron one-photon (TEOP) transitions to the ground state with the emission of a single $K_{\alpha\alpha}$ photon in a He-like sequence of atomic ions: from boron to uranium. The corresponding transition probabilities and transition energies are calculated within the QED theory. The calculations of the transition probabilities are performed in various gauges. The intensity ratios between the TEOP transitions and the other major transitions are presented.

DOI: 10.1103/PhysRevA.104.012818

I. INTRODUCTION

The autoionizing states are responsible for many resonant processes in the collision of highly charged ions with electrons and other atomic particles. Such resonant processes as dielectronic and trielectronic recombinations [1], excitation autoionization [2], and resonant excitation double autoionization [3] actively proceed in highly ionized laboratory and astrophysical plasmas. The resonance structure of these collision processes is mainly determined by the autoionizing states. Therefore, they continue to trigger the interest of researchers working in different fields of physics from both experimental and theoretical points of view.

The autoionizing states are of particular interest for studying two-electron one-photon (TEOP) transitions, which are single-photon transitions where two electrons change their quantum numbers. Such transitions occur only due to the interelectron interaction and represent a process that is very sensitive to the description of the interelectron correlation.

In the present work, we perform the calculation of the TEOP transition probabilities for He-like ions within the QED theory. The calculations of these transition probabilities were presented in [4–10]. The investigations of transitions, where both electrons change their principal quantum numbers, were presented in [4–7] for $Z \leqslant 47$. The calculations of the probabilities for transitions from autoionizing states to single excited states, $(2s^2) \to (1s, 2p)$, are presented in [6,8–10]. In the works [4,8], the calculations are performed within perturbation theory with respect to the interelectron interaction [11,12]; in the works [5–7,10], the calculations are performed with the use of the GRASP program [13,14].

The first successful experimental investigation of the TEOP transitions was reported in work [15], where two vacancies in a K shell were filled by two LL electrons with single-photon emission observed in Ni-Ni, Ni-Fe, Fe-Ni, and Fe-Fe collisions. In works [16,17], TEOP transitions $(2s^2) \to (1s, 2p)$ and $(1s, 2s^2) \to (1s^2, 2p)$ in He- and Li-like ions of Si were investigated experimentally. In work [18], the TEOP transition $(1s, 2s^2) \to (1s^2, 2p)$ was investigated experimentally in the process of dielectronic recombination with He-like Ar. In the recent work [19], the strong TEOP $[(1s2s)_1 5p]_{1/2,3/2} \to 1s^2 4s$ transition was observed in Li-like ions of O.

We consider the TEOP decay of LL autoionizing states of He-like ions to its ground state, where both electrons change their principal quantum numbers. The most attention is paid to the $(2s2p_{1/2})_1 \to 1s^2$ and $(2s2p_{3/2})_1 \to 1s^2$ transitions, which represent the strongest ones with $K_{\alpha\alpha}$ emission. The TEOP transitions in the lowest order of the QED perturbation theory are described by the Feynman graphs depicted in Fig. 1. In particular, the $(2s2p) \to (1s)^2 + \gamma$ transition is represented by these Feynman graphs, where $(ab) = (2s2p)$ and $(a'b') = (1s1s)$. In this case, the initial state is an autoionizing state and, in the summation over the complete Dirac spectrum, there are intermediate continuum states (e_n) with the energies $\varepsilon_n > m_e c^2$ such that $\varepsilon_{2s} + \varepsilon_{2p} \approx \varepsilon_{1s} + \varepsilon_{e_n}$. For the TEOP transitions, such states are of importance since they participate in a channel of the $(2s2p) \to (1s, e_n) \to (1s)^2 + \gamma$ decay. In order to take into account the region of these states, a special method was developed. This region of the continuum states is absent in the previous calculations using GRASP [5,6].

*k.n.lyashenko@impcas.ac.cn

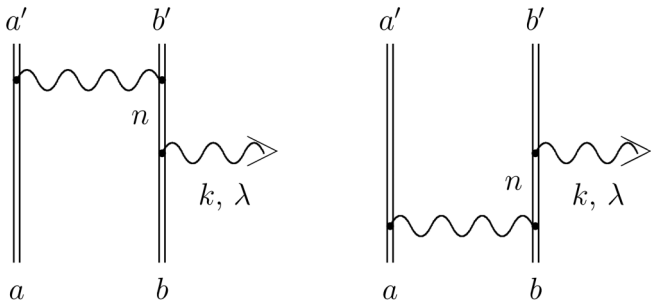

FIG. 1. The Feynman graphs corresponding to the lowest order of the QED perturbation theory contributing to the TEOP transitions with one-photon emission, where k and λ are 4-momentum and polarization of the photon, respectively. The index n denotes the summation and integration over the complete Dirac spectrum.

Below, we present the exact QED method for calculating the TEOP transition probabilities and analyze the numerical results.

II. METHOD OF CALCULATIONS

The autoionizing states are usually quasidegenerate. Accordingly, the quasidegenerate QED perturbation theory should be used for the description of the TEOP transitions. For this purpose, we use the line-profile approach (LPA) [20,21]. Within the LPA, the reference states (the initial and final states) are associated with certain positions of resonances in some process of scattering (usually the photon scattering is considered). The positions of the resonances depend on the properties of the scattering process. In order to describe the reference states by only two parameters (the energy and width), it is necessary to use an approximation—the resonant approximation. In this approximation, the line profile is interpolated by a Lorentz profile which is characterized by the position of resonance and its width.

For the application of the quasidegenerate perturbation theory within the LPA, the infinite matrix $V = V^{(0)} + \Delta V$ is introduced. The matrix $V^{(0)}$ is a diagonal matrix and its matrix elements have the following form:

$$(V^{(0)})_{ud} = \left\langle \Psi_u^{(0)}(\boldsymbol{r}_1, \boldsymbol{r}_2) \middle| \hat{h}_{\boldsymbol{r}_1} + \hat{h}_{\boldsymbol{r}_2} \middle| \Psi_d^{(0)}(\boldsymbol{r}_1, \boldsymbol{r}_2) \right\rangle, \quad (1)$$

where indices $u = (J_u M_u, u_1, u_2)$ and $d = (J_d M_d, d_1, d_2)$ represent complete sets of the quantum numbers describing two-electron states, and $u_i = (n_{u_i} j_{u_i} l_{u_i})$ and $d_i = (n_{d_i} j_{d_i} l_{d_i})$ denote sets of the quantum numbers describing one-electron states (n, j, and l are the principal quantum number, the total angular momentum, and the orbital angular momentum, respectively). The two-electron wave functions $\Psi_n^{(0)}$ in the j-j coupling scheme read

$$\Psi_n^{(0)}(\boldsymbol{r}_1, \boldsymbol{r}_2) = N \sum_{m_{n_1} m_{n_2}} C_{J_n M_n}^{j_{n_1} j_{n_2}}(m_{n_1} m_{n_2}) \times \det\left\{\psi_{n_1}(\boldsymbol{r}_1), \psi_{n_2}(\boldsymbol{r}_2)\right\}, \quad (2)$$

where $C_{J_n M_n}^{j_{n_1} j_{n_2}}(m_{n_1} m_{n_2})$ are the Clebsch-Gordan coefficients, N is a normalization constant, and ψ_{n_1} and ψ_{n_2} are the one-electron Dirac wave functions corresponding to energies ε_{n_1} and ε_{n_2}. In Eq. (1), $\hat{h}_{\boldsymbol{r}} = \boldsymbol{\alpha}\hat{\boldsymbol{p}} + \beta - \frac{\alpha Z}{r}$ is the Dirac Hamiltonian, α is the fine structure constant, and β, $\boldsymbol{\alpha}$ are the Dirac matrices. The relativistic units ($\hbar = c = m_e = 1$) are used throughout, unless otherwise stated.

Matrix ΔV contains a small parameter of the QED perturbation theory. In the present work, ΔV is formed by the matrix elements of the one- and two-photon exchange corrections, the electron self-energy, and vacuum polarization corrections. For the considered process, the most important correction is the one-photon exchange. The matrix elements of ΔV corresponding to this correction are expressed as

$$(\Delta V^{1\mathrm{ph}})_{ud} = \alpha \left\langle \Psi_u^{(0)}(\boldsymbol{r}_1, \boldsymbol{r}_2) \middle| \alpha^{\nu_1} \alpha^{\nu_2} I_{\nu_1 \nu_2}\left(\left|\varepsilon_{u_1} - \varepsilon_{d_1}\right|, r_{12}\right) \times \middle| \Psi_d^{(0)}(\boldsymbol{r}_1, \boldsymbol{r}_2) \right\rangle, \quad (3)$$

where $\alpha^{\nu} = (1, \boldsymbol{\alpha})$, and $I_{\nu_1 \nu_2}$ denotes the photon propagator which, in the Feynman gauge, is given by

$$I_{\nu_1 \nu_2}(\Omega, r_{12}) = \frac{g_{\nu_1 \nu_2} \exp(i\Omega r_{12})}{r_{12}}, \quad (4)$$

where $r_{12} = |\boldsymbol{r}_1 - \boldsymbol{r}_2|$, and $g_{\nu_1 \nu_2} = (1, -1, -1, -1)$ is the metric tensor. The other corrections such as two-photon exchange corrections, the electron self-energy, and vacuum polarization corrections are taken into account in a similar way [20].

Following LPA, we introduce the finite set of two-electron configurations (g), which includes all the two-electron configurations composed of a certain set of electrons (for example, $1s$, $2s$, $2p$, $3s$, $3p$, $3d$ electrons). The set g should include configurations with energies close to the energy of a reference state n_g, which is the initial or final state of the considered process. The matrix V can be presented as a block matrix [20],

$$V = \begin{bmatrix} V_{11} & V_{12} \\ V_{21} & V_{22} \end{bmatrix} = \begin{bmatrix} V_{11}^{(0)} + \Delta V_{11} & \Delta V_{12} \\ \Delta V_{21} & V_{22}^{(0)} + \Delta V_{22} \end{bmatrix} \quad (5)$$

where matrix V_{11} is defined on the set g, which contains configurations mixing with the reference state $n_g \in g$. Matrix V_{11} is a finite matrix and can be diagonalized numerically,

$$V_{11}^{\mathrm{diag}} = B^t V_{11} B, \quad B^t B = I. \quad (6)$$

Then, the standard perturbation theory can be applied for the diagonalization of the infinite matrix V. The initial and final states are described by the corresponding eigenvectors of this matrix [20],

$$\Phi_{n_g} = \sum_{k_g \in g} B_{k_g n_g} \Psi_{k_g}^{(0)} + \sum_{k \notin g, l_g \in g} [\Delta V]_{k l_g} \times \frac{B_{l_g n_g}}{E_{n_g} - E_k^{(0)}} \Psi_k^{(0)} + \cdots, \quad (7)$$

where $n_g = (JM, n_1 j_1 l_1, n_2 j_2 l_2)$ is a complete set of quantum numbers describing the reference state, and indices k, l_g describe the two-electron configurations: the index l_g runs over all configurations of the set g; the index k runs over all the configurations not included in the set g (this implies integration over the positive- and negative-energy continuum). Here, the two-electron wave functions $\Psi_n^{(0)}$ are the Slater determinants in the j-j coupling scheme, and the corresponding energies $E_n^{(0)}$ are the sum of the one-electron Dirac energies. The energies E_{n_g} are the eigenvalues of the matrix V_{11}.

The first term in Eq. (7) corresponds to the zeroth order of the quasidegenerate perturbation theory and describes the

correlation between the configurations included in the set g, which is expressed in the matrix B. The second term in Eq. (7) determines the first order of the quasidegenerate perturbation theory and describes the correlation of the reference state with all other configurations which are not included in the set g. We note that the set g is chosen so that the denominators in Eq. (7) are large enough for the convergence of the perturbation theory. Both terms take into account the higher-order corrections of the standard QED perturbation theory. For regular transitions, if the set g is large enough, the first term provides high accuracy. However, in the case of special transitions such as TEOP, the second term can make a significant contribution to the transition probabilities and should be taken into account.

If the reference state n_g is an autoionizing state, then in the continuous part of the Dirac spectrum there is a one-electron state with the energy such that the corresponding two-electron energy $E_k^{(0)}$ is close to E_{n_g}. This leads to an appearance of small values in the denominator in Eq. (7). During the integration over the continuous part of the spectrum, we can see considerable cancellation in the contributions of the energy regions below and above E_{n_g}. We note that the autoionizing states have nonzero widths ($\Gamma_{n_g} = -2\mathrm{Im}\{E_{n_g}\}$), and there is no divergence in the integration over the continuous part of the Dirac spectrum.

In the present work, the summation over the complete Dirac spectrum was performed using a finite basis set for the Dirac equation constructed from B-splines [22,23]. The size of the basis set is chosen as $N \approx 100$. In the framework of this method, the ion is considered enclosed within a sphere with the finite radius $R \approx 100/(\alpha Z)$ r.u. Accordingly, the Dirac spectrum (ε_n) is replaced by a finite number of pseudostates (with energies $\varepsilon_n^{(R,N)}$) for fixed angular quantum numbers: N positive-energy states and N negative-energy states [22]. The low-lying positive-energy states accurately describe the corresponding Dirac states ($\varepsilon_n \approx \varepsilon_n^{(R,N)}$). The B-spline states with energies $\varepsilon_n^{(R,N)} > m_e c^2$ and $\varepsilon_n^{(R,N)} < -m_e c^2$ do not describe physical states, but describe the B-spline approximation of the continuum part of the Dirac spectrum. These B-spline states significantly depend on both the radius R and the size of the basis N. The corresponding two-electron energies $E_n^{(R,N)}$ also depend on R and N. Hence, the denominators in Eq. (7) continuously depend on R. We note that if the reference state is not an autoionizing state, then the result of the summation does not depend on R. However, in the case of the autoionizing states, special attention should be paid to the energy region in which the denominator becomes small and the considerable cancellation mentioned above takes place. The implementation of this cancellation can be done in two ways. The first one is to adjust the radius R so that $\mathrm{Re}\{E_{n_g}\} = (E_n^{(R,N)} + E_{n+1}^{(R,N)})/2$. The cancellation between the n and $n+1$ terms implements the mentioned cancellation in the continuous part of the Dirac spectrum. This approach was successfully used in [24] for calculation of the energy levels of autoionizing states. The second way is to adjust the radius R so that $\mathrm{Re}\{E_{n_g}\} = E_n^{(R,N)}$ and to exclude the corresponding term from the summation. In this case, the cancellation between $n-1$ and $n+1$ takes place. In the present work, we used the second approach. We found that the second method is more convenient for dealing with complex values. The result of the summation is stable for R and N if the appropriate fine adjustment procedure is followed.

The amplitude of the one-photon transition is given as a matrix element of the photon emission operator ($\hat{\Xi}$), with the bra and ket vectors given by the functions Φ in Eq. (7) corresponding to the initial and final states, respectively,

$$U_{\mathrm{if}} = \langle \Phi^{\mathrm{fin}} | \hat{\Xi} | \Phi^{\mathrm{ini}} \rangle. \tag{8}$$

The operator $\hat{\Xi}$ is constructed using perturbation theory [20,21]. In this work, we consider this operator in the zeroth order. The contribution of the first order is small and can be neglected [21]. The zeroth order of operator $\hat{\Xi}$ can be represented by its matrix elements which read

$$\Xi^{(0)}_{u_1 u_2 d_1 d_2} = e A^{(k,\lambda)*}_{u_1 d_1} \delta_{u_2 d_2} + e A^{(k,\lambda)*}_{u_2 d_2} \delta_{u_1 d_1}, \tag{9}$$

where u_1, u_2, d_1, d_2 are one-electron states with certain total angular momentum and parity, and the one-electron matrix elements $A^{(k,\lambda)*}_{ud}$ are defined as

$$A^{(k,\lambda)*}_{ud} = \int d^3\boldsymbol{r}\, \overline{\psi}_u(\boldsymbol{r}) \gamma^\nu A^{(k,\lambda)*}_\nu(\boldsymbol{r}) \psi_d(\boldsymbol{r}). \tag{10}$$

The photon wave function $A^{(k,\lambda)\nu} = (V^{(k,\lambda)}, \boldsymbol{A}^{(k,\lambda)})$ in the velocity (transverse) gauge can be written as

$$V^{(k,\lambda)}(\boldsymbol{r}) = 0, \quad \boldsymbol{A}^{(k,\lambda)}(\boldsymbol{r}) = \sqrt{\frac{2\pi}{\omega}} e^{i\boldsymbol{k}\boldsymbol{r}} \boldsymbol{e}^{(\lambda)}, \tag{11}$$

where $\boldsymbol{k}$ is the photon wave vector, $\omega = |\boldsymbol{k}|$ is the frequency, and $\boldsymbol{e}^{(\lambda)}$ is the polarization vector with the polarization λ. For the description of autoionizing states, the quasidegenerate QED perturbation theory is utilized. In particular, we partly take into account the higher orders of the standard QED perturbation theory. In the general case, this leads to a violation of gauge invariance for a fixed order of the quasidegenerate QED perturbation theory. The violation of gauge invariance is explained by the higher-order corrections [20] and can be used to estimate the contribution of the higher orders of the employed perturbation theory.

We also use the following gauge transformation for the photon wave function in Eq. (11):

$$V^{(k,\lambda)} = G \sqrt{\frac{2\pi}{\omega}} e^{i\boldsymbol{k}\boldsymbol{r}}, \tag{12}$$

$$\mathbf{A}^{(k,\lambda)} = (\boldsymbol{e}^{(\lambda)} + G\boldsymbol{v}) \sqrt{\frac{2\pi}{\omega}} e^{i\boldsymbol{k}\boldsymbol{r}}, \tag{13}$$

where $\boldsymbol{v} = \boldsymbol{k}/\omega$ and G is an arbitrary gauge parameter which is set equal to $G = 1$. The velocity gauge is given by $G = 0$.

The transition probability is connected with the amplitude as

$$dW_{\mathrm{if}} = 2\pi \delta(E_i - E_f) \left| U^{(k,\lambda)}_{\mathrm{if}} \right|^2 \frac{d^3\boldsymbol{k}}{(2\pi)^3}, \tag{14}$$

where E_i and E_f are the energies of the initial and final states of the system, respectively. The total transition probability involves the integration over the photon momentum ($\boldsymbol{k}$), the summation over the photon polarizations (λ), the averaging over the projections of the total angular momentum of the initial state (M_i), and summation over the projections of the

final state (M_f),

$$W_{\rm if} = \frac{1}{2J_i+1}\sum_{M_i,M_f}\frac{\omega^2}{(2\pi)^2}\int d^2\boldsymbol{\nu}\sum_{\lambda}\left|U_{\rm if}^{(k,\lambda)}\right|^2. \quad (15)$$

The integration over $\boldsymbol{k}$ and the summation over λ can be performed analytically [25]. For this purpose, the wave functions of the photons with certain k and λ are expressed in terms of the wave functions of the photons with certain angular momentum (j), its projection (m), and type of photons (electric photons [$\xi = 1$] and magnetic photons [$\xi = 0$]). After the integration over $\boldsymbol{k}$ and the summation over λ, the total transition probability can be written as

$$W_{\rm if} = \frac{\omega^2}{(2\pi)^2}\sum_{jl\xi}\left|U_{\rm if}^{(j,l,\xi)}\right|^2, \quad (16)$$

where the expression for $U_{\rm if}^{(j,l,\xi)}$ is given by Eqs. (8)–(10) where, in Eq. (10), the 4-vector $A^{(k,\lambda)\nu}$ is substituted by $A_{jm}^{({\rm E,M})\nu} = (V_{jm}^{({\rm E,M})}, \mathbf{A}_{jm}^{({\rm E,M})})$. The magnetic photon wave functions read

$$V_{jm}^{\rm M}(\boldsymbol{r},\omega) = 0, \quad (17)$$

$$\boldsymbol{A}_{jm}^{\rm M}(\boldsymbol{r},\omega) = \sqrt{\frac{2\pi}{\omega}}g_j(\omega r)\boldsymbol{Y}_{jjm}(\boldsymbol{n}), \quad (18)$$

where $g_j(x) = 4\pi j_j(x)$, $j_j(x)$ is the spherical Bessel function [26], and $\boldsymbol{Y}_{jlm}(\boldsymbol{n})$ denotes the vector spherical harmonics [27] depending on angles $\boldsymbol{n} = \boldsymbol{r}/|\boldsymbol{r}|$. The electric photon wave functions in the velocity gauge are

$$V_{jm}^{\rm E}(\boldsymbol{r},\omega) = 0, \quad (19)$$

$$\boldsymbol{A}_{jm}^{\rm E}(\boldsymbol{r},\omega) = \sqrt{\frac{2\pi}{\omega}}\left\{\sqrt{\frac{j}{2j+1}}g_{j+1}(\omega r)\boldsymbol{Y}_{jj+1m}(\boldsymbol{n}) - \sqrt{\frac{j+1}{2j+1}}g_{j-1}(\omega r)\boldsymbol{Y}_{jj-1m}(\boldsymbol{n})\right\}. \quad (20)$$

For investigation of the gauge invariance, the results of the calculation in the velocity (transverse) gauge are compared with the ones obtained in the length (nontransverse) gauge. The length gauge can be derived from the velocity gauge by the following transformation in the momentum representation: $\boldsymbol{A} \to \boldsymbol{A} + \boldsymbol{\nu}\chi(\boldsymbol{k},t)$, $V \to V + \chi(\boldsymbol{k},t)$, with

$$\chi(\boldsymbol{k},t) = \delta(\omega - |\boldsymbol{k}|)\sqrt{\frac{j+1}{j}}Y_{jm}(\boldsymbol{\nu})e^{-i\omega t}, \quad (21)$$

where $Y_{jm}(\boldsymbol{\nu})$ is the spherical harmonics [27]. This transformation affects only the electric photons. Accordingly, in the length gauge, the 4-vector $A_{jm}^{({\rm E})\nu}$ appears as

$$V_{jm}^{\rm E}(\boldsymbol{r},\omega) = -\sqrt{\frac{2\pi}{\omega}}\sqrt{\frac{j+1}{j}}g_j(\omega r)Y_{jm}(\boldsymbol{n}), \quad (22)$$

$$\boldsymbol{A}_{jm}^{({\rm E})}(\boldsymbol{r},\omega) = \sqrt{\frac{2\pi}{\omega}}\sqrt{\frac{2j+1}{j}}g_{j+1}(\omega r)\boldsymbol{Y}_{jj+1m}(\boldsymbol{n}). \quad (23)$$

To analyze the obtained results, we also performed calculations taking into account only the first term in Eq. (7). This corresponds to the zeroth order of quasidegenerate perturbation theory. The zeroth-order transition probabilities are denoted as W_0.

III. RESULTS AND DISCUSSION

We consider TEOP transitions from autoionizing LL states to the ground state of He-like ions. In Table I, we present the corresponding transition probabilities for the states with nonzero total angular momentum ($J \neq 0$) for He-like ions of boron, neon, argon, krypton, xenon, tungsten, and uranium (states with $J = 0$ do not decay to the ground state by one-photon emission). In the first column, the initial states are indicated. The second and third columns give the energies (E) and the total widths (Γ) of the initial states. The calculation takes into account the one- and two-photon exchange corrections as well as the electron self-energy and vacuum polarization corrections. The higher-order corrections are also partly taken into account. The total widths (Γ) of the autoionizing states include both the radiative and Auger widths. The fourth column presents the energies of the emitted photons. In the next six columns, we present the transition probabilities calculated within three gauges: velocity gauge ($W_0^{({\rm V})}$ and $W^{({\rm V})}$), length gauge ($W_0^{({\rm L})}$ and $W^{({\rm L})}$), and gauge with $G = 1$ ($W_0^{(G=1)}$ and $W^{(G=1)}$). The gauge parameter G is introduced in Eqs. (12) and (13). The values $W_0^{({\rm V})}$, $W_0^{({\rm L})}$, and $W_0^{(G=1)}$ correspond to the calculations performed within the framework of the zeroth order of the quasidegenerate perturbation theory, while $W^{({\rm V})}$, $W^{({\rm L})}$, and $W^{(G=1)}$ correspond to the full calculation [see Eq. (7)]. We note that the considered gauges make it possible to check the gauge invariance of the electric transitions, while the magnetic transitions remain unchanged. Therefore, the magnetic-transition probabilities are given in only one gauge in Table I. To compare the intensities of the TEOP transitions with those for other transitions, we present the branching ratio $\Gamma_{\rm TEOP}/\Gamma$ and the intensity ratio $\Gamma_{\rm TEOP}/\Gamma_{\rm OEOP}$, where $\Gamma_{\rm TEOP}$ is related to the TEOP transition probability as $\Gamma_{\rm TEOP} = \hbar W^{({\rm V})}$ and $\Gamma_{\rm OEOP}$ denotes the radiative widths corresponding to all possible one-electron one-photon (OEOP) transitions.

The difference between W_0 and W shows the importance of the first order of the quasidegenerate perturbation theory. The individual contributions of the zeroth and first orders can vary greatly in different gauges. The application of the quasidegenerate perturbation theory leads to the violation of gauge invariance since the calculations partly take into account the higher orders of the interelectron interaction. Accordingly, the results of the full calculations may be gauge dependent. The difference between the full calculations in the considered gauges can be used to estimate the calculation accuracy, which is determined by the higher-order contributions of the used perturbation theory. The interelectron interaction is more important for light ions than for heavy ones. Therefore, the used perturbation theory works better for heavier ions. Moreover, the convergence of the perturbation theory may be different for various gauges and for various transitions. In particular, for uranium ion, the relative differences between results in various gauges are $\leqslant 0.1\%$ and $\leqslant 1.8\%$ for the E1 transitions from the $(2s2p_{3/2})_1$ and $(2s2p_{1/2})_1$ states, respectively, and

TABLE I. The TEOP transition probabilities to the ground state for LL states of He-like ions. The first column indicates the LL states. The second and third columns present the energies ΔE ($\Delta E = E - 2m_e c^2$, where E is the full energy of the state) and total widths Γ of the corresponding states. Column 4 gives the transition energies (ω). The next six columns present the TEOP transition probabilities to the ground state calculated in the three different gauges: velocity gauge ($W_0^{(\mathrm{V})}$ and $W^{(\mathrm{V})}$), length gauge ($W_0^{(\mathrm{L})}$ and $W^{(\mathrm{L})}$), and gauge with $G = 1$ [$W_0^{(G=1)}$ and $W^{(G=1)}$; see Eqs. (12) and (13)]. Subscript 0 at W_0 denotes that the calculation was performed within the zeroth order [the first term in Eq. (7)], while values without this subscript correspond to the full calculation. The last two columns contain the branching ratio $\Gamma_{\mathrm{TEOP}}/\Gamma$ and the intensity ratio $\Gamma_{\mathrm{TEOP}}/\Gamma_{\mathrm{OEOP}}$, where $\Gamma_{\mathrm{TEOP}} = \hbar W^{(\mathrm{V})}$ and Γ_{OEOP} is the radiative width corresponding to all of the one-electron one-photon transitions.

Initial state	ΔE (keV)	Γ (eV)	ω (keV)	$W_0^{(\mathrm{V})}$ (s^{-1})	$W^{(\mathrm{V})}$ (s^{-1})	$W_0^{(\mathrm{L})}$ (s^{-1})	$W^{(\mathrm{L})}$ (s^{-1})	$W_0^{(G=1)}$ (s^{-1})	$W^{(G=1)}$ (s^{-1})	$\frac{\Gamma_{\mathrm{TEOP}}}{\Gamma}$	$\frac{\Gamma_{\mathrm{TEOP}}}{\Gamma_{\mathrm{OEOP}}}$
					$Z = 5$						
$(2s2p_{1/2})_1$	−0.15275	0.008	0.44666	1.632 [4]	1.202 [4]	5.607 [3]	1.288 [4]	1.771 [4]	1.202 [4]	9.72 [−10]	3.29 [−8]
$(2s2p_{3/2})_1$	−0.14626	0.110	0.45315	3.106 [9]	2.037 [9]	1.161 [9]	2.422 [9]	3.341 [9]	2.045 [9]	1.22 [−5]	5.51 [−3]
$(2s2p_{3/2})_2$	−0.15274	0.008	0.44667	1.901 [2]	6.974 [1]					5.71 [−12]	1.91 [−10]
$(2p_{1/2}2p_{3/2})_1$	−0.14878	<0.001	0.45063	5.735 [−2]	2.131 [−2]					2.95 [−14]	2.95 [−14]
$(2p_{1/2}2p_{3/2})_2$	−0.14687	0.203	0.45253	4.186 [1]	3.314 [4]	7.383 [5]	2.326 [3]	4.849 [5]	4.516 [4]	1.08 [−10]	4.68 [−8]
$(2p_{3/2})_2^2$	−0.14876	<0.001	0.45065	2.739 [−3]	1.145 [0]	2.839 [1]	2.786 [−2]	1.856 [1]	1.692 [0]	1.56 [−12]	1.59 [−12]
					$Z = 10$						
$(2s2p_{1/2})_1$	−0.64577	0.013	1.91214	3.203 [6]	2.283 [6]	1.032 [6]	2.500 [6]	3.502 [6]	2.285 [6]	1.15 [−7]	3.77 [−7]
$(2s2p_{3/2})_1$	−0.63129	0.126	1.92662	1.332 [10]	9.145 [9]	4.872 [9]	1.028 [10]	1.436 [10]	9.162 [9]	4.79 [−5]	1.50 [−3]
$(2s2p_{3/2})_2$	−0.64548	0.013	1.91243	1.573 [4]	5.517 [3]					2.89 [−10]	9.12 [−10]
$(2p_{1/2}2p_{3/2})_1$	−0.63727	0.008	1.92064	1.950 [1]	8.084 [0]					6.70 [−13]	6.70 [−13]
$(2p_{1/2}2p_{3/2})_2$	−0.63244	0.232	1.92547	3.171 [1]	9.643 [5]	1.399 [7]	6.655 [5]	9.299 [6]	9.827 [5]	2.74 [−9]	8.05 [−8]
$(2p_{3/2})_2^2$	−0.63702	0.008	1.92089	2.906 [−1]	1.759 [3]	2.786 [4]	1.157 [3]	1.846 [4]	1.801 [3]	1.38 [−10]	1.46 [−10]
					$Z = 18$						
$(2s2p_{1/2})_1$	−2.14979	0.054	6.39711	3.001 [8]	2.154 [8]	9.934 [7]	2.309 [8]	3.272 [8]	2.155 [8]	2.62 [−6]	3.33 [−6]
$(2s2p_{3/2})_1$	−2.12077	0.169	6.42613	4.536 [10]	3.203 [10]	1.638 [10]	3.465 [10]	4.898 [10]	3.206 [10]	1.25 [−4]	4.96 [−4]
$(2s2p_{3/2})_2$	−2.14655	0.052	6.40035	6.256 [5]	2.148 [5]					2.74 [−9]	3.34 [−9]
$(2p_{1/2}2p_{3/2})_1$	−2.13149	0.085	6.41541	2.408 [3]	1.114 [3]					8.65 [−12]	8.65 [−12]
$(2p_{1/2}2p_{3/2})_2$	−2.12912	0.100	6.41777	9.075 [0]	6.881 [5]	1.142 [7]	5.986 [5]	7.600 [6]	6.902 [5]	4.53 [−9]	5.35 [−9]
$(2p_{3/2})_2^2$	−2.12024	0.302	6.42666	1.968 [1]	1.031 [7]	1.611 [8]	9.061 [6]	1.074 [8]	1.033 [7]	2.25 [−8]	8.04 [−8]
					$Z = 36$						
$(2s2p_{1/2})_1$	−8.86672	0.725	26.36484	2.887 [10]	2.110 [10]	9.840 [9]	2.198 [10]	3.137 [10]	2.110 [10]	1.91 [−5]	2.01 [−5]
$(2s2p_{3/2})_1$	−8.75552	0.792	26.47603	1.761 [11]	1.287 [11]	6.561 [10]	1.346 [11]	1.894 [11]	1.288 [11]	1.07 [−4]	1.25 [−4]
$(2s2p_{3/2})_2$	−8.80072	0.687	26.43083	4.914 [7]	1.659 [7]					1.59 [−8]	1.62 [−8]
$(2p_{1/2}2p_{3/2})_1$	−8.77044	1.367	26.46111	6.209 [5]	3.995 [5]					1.92 [−10]	1.92 [−10]
$(2p_{1/2}2p_{3/2})_2$	−8.75962	1.495	26.47193	1.119 [4]	5.287 [7]	2.045 [9]	5.000 [7]	1.360 [9]	5.290 [7]	2.33 [−8]	2.55 [−8]
$(2p_{3/2})_2^2$	−8.68575	1.453	26.54580	7.193 [3]	4.899 [7]	1.628 [9]	4.659 [7]	1.085 [9]	4.901 [7]	2.22 [−8]	2.39 [−8]
					$Z = 54$						
$(2s2p_{1/2})_1$	−20.6452	3.617	60.9258	1.592 [11]	1.174 [11]	6.277 [10]	1.202 [11]	1.703 [11]	1.175 [11]	2.14 [−5]	2.18 [−5]
$(2s2p_{3/2})_1$	−20.1851	3.463	61.3858	3.832 [11]	2.922 [11]	1.798 [11]	3.032 [11]	4.024 [11]	2.923 [11]	5.55 [−5]	5.73 [−5]
$(2s2p_{3/2})_2$	−20.2494	3.372	61.3215	6.773 [8]	2.333 [8]					4.55 [−8]	4.57 [−8]
$(2p_{1/2}2p_{3/2})_1$	−20.2048	6.906	61.3662	1.416 [7]	1.513 [7]					1.44 [−9]	1.44 [−9]
$(2p_{1/2}2p_{3/2})_2$	−20.1889	7.051	61.3821	3.555 [5]	1.133 [8]	1.537 [10]	1.108 [8]	1.026 [10]	1.135 [8]	1.06 [−8]	1.08 [−8]
$(2p_{3/2})_2^2$	−19.7764	6.784	61.7946	2.214 [5]	8.396 [7]	7.735 [9]	8.788 [7]	5.143 [9]	8.416 [7]	8.15 [−9]	8.24 [−9]
					$Z = 74$						
$(2s2p_{1/2})_1$	−40.9132	12.88	119.0230	4.970 [11]	3.557 [11]	2.590 [11]	3.549 [11]	5.167 [11]	3.557 [11]	1.82 [−5]	1.84 [−5]
$(2s2p_{3/2})_1$	−39.2130	11.54	120.7232	7.868 [11]	6.404 [11]	5.573 [11]	6.451 [11]	7.978 [11]	6.405 [11]	3.65 [−5]	3.69 [−5]
$(2s2p_{3/2})_2$	−39.3046	11.45	120.6316	5.565 [9]	2.064 [9]					1.19 [−7]	1.19 [−7]
$(2p_{1/2}2p_{3/2})_1$	−39.2494	24.16	120.6868	1.191 [8]	2.767 [8]					7.54 [−9]	7.54 [−9]
$(2p_{1/2}2p_{3/2})_2$	−39.2314	24.30	120.7048	1.390 [7]	1.508 [9]	6.266 [10]	1.413 [9]	4.277 [10]	1.510 [9]	4.09 [−8]	4.11 [−8]
$(2p_{3/2})_2^2$	−37.5940	22.89	122.3422	2.376 [6]	5.995 [8]	2.544 [10]	5.666 [8]	1.687 [10]	6.001 [8]	1.72 [−8]	1.73 [−8]
					$Z = 92$						
$(2s2p_{1/2})_1$	−67.8558	31.34	193.5296	1.152 [12]	7.454 [11]	7.639 [11]	7.320 [11]	1.174 [12]	7.454 [11]	1.57 [−5]	1.58 [−5]
$(2s2p_{3/2})_1$	−63.2680	26.19	198.1173	1.386 [12]	1.213 [12]	1.481 [12]	1.215 [12]	1.389 [12]	1.213 [12]	3.05 [−5]	3.06 [−5]
$(2s2p_{3/2})_2$	−63.3917	26.06	197.9936	2.559 [10]	1.066 [10]					2.69 [−7]	2.70 [−7]
$(2p_{1/2}2p_{3/2})_1$	−63.3554	56.91	198.0300	4.181 [8]	2.280 [9]					2.64 [−8]	2.64 [−8]
$(2p_{1/2}2p_{3/2})_2$	−63.3397	57.03	198.0456	2.367 [8]	1.217 [10]	1.363 [11]	1.171 [10]	9.821 [10]	1.218 [10]	1.40 [−7]	1.41 [−7]
$(2p_{3/2})_2^2$	−58.8286	51.94	202.5567	8.687 [6]	3.978 [9]	4.379 [10]	3.813 [9]	2.895 [10]	3.980 [9]	5.04 [−8]	5.05 [−8]

TABLE II. The transition probabilities for the $(2s2p_{3/2})_1$ state of the He-like sequence of atomic ions. The first column presents atomic number Z of the ion; the second and third columns present the energies ΔE ($\Delta E = E - 2m_e c^2$, where E is the full energy of the state) and widths Γ of the $(2s2p_{3/2})_1$ state. Columns 4 and 5 correspond to TEOP transitions to the ground state, where ω is the transition energy and W is the TEOP transition probability in the velocity gauge. Further, columns 6 and 7 contain the branching ratio $\Gamma_{\rm TEOP}/\Gamma$ and the intensity ratio $\Gamma_{\rm TEOP}/\Gamma_{\rm OEOP}$. The last four columns correspond to transitions with final $(1s2s)_0$ and $(1s2s)_1$ states, where ω is the transition energy and W is the OEOP transition probability. The values marked by superscript letters a–e are taken from works [4], [5], [6], [8], and [7], respectively.

	Initial state		Final state							
	$(2s2p_{3/2})_1$		$(1s)^2$				$(1s2s)_0$		$(1s2s)_1$	
Z	ΔE (keV)	Γ (eV)	ω (keV)	W (s^{-1})	$\frac{\Gamma_{\rm TEOP}}{\Gamma}$	$\frac{\Gamma_{\rm TEOP}}{\Gamma_{\rm OEOP}}$	ω (keV)	W (s^{-1})	ω (keV)	W (s^{-1})
5	−0.14626	0.110	0.45315	2.04 [9]	1.22 [−5]	5.51 [−3]	0.25034	3.51 [11]	0.25470	1.06 [6]
			0.45294[a]	2.64[9][a]			0.25015[a]	3.58[11][a]		
			0.452658[b]	1.268[9][b]				3.517[11][b]		9.442[5][b]
6	−0.21599	0.114	0.66595	3.03 [9]	1.75 [−5]	3.92 [−3]	0.36156	7.44 [11]	0.36709	6.30 [6]
			0.665436[b]	1.703[9][b]				7.459[11][b]		6.045[6][b]
							0.36135[d]	7.57[11][d]	0.36677[d]	8.17[6][d]
7	−0.29934	0.118	0.91965	4.24 [9]	2.36 [−5]	2.94 [−3]	0.49325	1.40 [12]	0.49995	2.94 [7]
			0.919113[b]	2.409[9][b]				1.401[12][b]		2.880[7][b]
							0.49304[d]	1.42[12][d]	0.49966[d]	3.69[7][d]
8	−0.39632	0.120	1.21431	5.66 [9]	3.09 [−5]	2.29 [−3]	0.64542	2.41 [12]	0.65332	1.11 [8]
			1.213744[b]	3.117[9][b]				2.413[12][b]		1.110[8][b]
							0.64523[d]	2.44[12][d]	0.65305[d]	1.37[8][d]
9	−0.50697	0.123	1.54995	7.29 [9]	3.90 [−5]	1.83 [−3]	0.81811	3.89 [12]	0.82721	3.64 [8]
			1.549366[b]	3.918[9][b]				3.893[12][b]		3.634[8][b]
							0.81792[d]	3.93[12][d]	0.82696[d]	4.35[8][d]
10	−0.63129	0.126	1.92662	9.15 [9]	4.79 [−5]	1.50 [−3]	1.0113	5.96 [12]	1.0216	1.05 [9]
			1.92666[a]	1.269[10][a]			1.01129[a]	6.00[12][a]		
			1.926027[b]	4.813[9][b]				5.964[12][b]		1.046[9][b]
			1.92600[e]	6.030[9][e]			1.01114[e]	5.661[12][e]	1.02197[e]	8.316[8][e]
							1.0112[d]	6.02[12][d]	1.0214[d]	1.22[9][d]
11	−0.76930	0.129	2.34438	1.12 [10]	5.74 [−5]	1.26 [−3]	1.2251	8.76 [12]	1.2367	2.73 [9]
12	−0.92103	0.132	2.80329	1.35 [10]	6.74 [−5]	1.07 [−3]	1.4595	1.25 [13]	1.4723	6.50 [9]
			2.802706[b]	6.899[9][b]				1.246[13][b]		6.466[9][b]
							1.4594[d]	1.26[13][d]	1.4721[d]	7.33[9][d]
13	−1.08650	0.136	3.30358	1.60 [10]	7.77 [−5]	9.17 [−4]	1.7147	1.72 [13]	1.7287	1.44 [10]
14	−1.26573	0.140	3.84505	1.88 [10]	8.81 [−5]	7.97 [−4]	1.9904	2.32 [13]	2.0057	3.00 [10]
			3.843901[b]	9.391[9][b]				2.318[13][b]		2.983[10][b]
			3.84442[e]	1.232[10][e]			1.99022[e]	2.237[13][e]	2.00604[e]	2.736[10][e]
							1.9903[d]	2.35[13][d]	2.0055[d]	3.31[10][d]
15	−1.45874	0.146	4.42791	2.17 [10]	9.82 [−5]	7.00 [−4]	2.2869	3.06 [13]	2.3035	5.92 [10]
			4.42864[a]	3.04[10][a]			2.28728[a]	3.09[13][a]		
16	−1.66556	0.152	5.05225	2.49 [10]	1.08 [−4]	6.20 [−4]	2.6043	3.96 [13]	2.6221	1.11 [11]
17	−1.88622	0.160	5.71817	2.84 [10]	1.17 [−4]	5.53 [−4]	2.9424	5.05 [13]	2.9615	2.01 [11]
18	−2.12077	0.169	6.42613	3.20 [10]	1.25 [−4]	4.96 [−4]	3.3017	6.35 [13]	3.3221	3.49 [11]
			6.424385[b]	1.568[10][b]				6.346[13][b]		3.465[11][b]
			6.42541[e]	2.077[10][e]			3.30140[e]	6.178[13][e]	3.32240[e]	3.318[11][e]
							3.3015[d]	6.47[13][d]	3.3219[d]	3.75[11][d]
19	−2.36920	0.179	7.17561	3.59 [10]	1.32 [−4]	4.48 [−4]	3.6818	7.88 [13]	3.7035	5.86 [11]
20	−2.63156	0.191	7.96702	4.00 [10]	1.38 [−4]	4.06 [−4]	4.0830	9.65 [13]	4.1060	9.53 [11]
			7.96916[a]	5.56[10][a]			4.08394[a]	9.84[13][a]		
			7.967522[b]	1.945[10][b]				9.646[13][b]		9.472[11][b]
			7.96643[e]	2.587[10][e]			4.08273[e]	9.419[13][e]	4.10639[e]	9.153[11][e]
							4.0828[d]	9.87[13][d]	4.1059[d]	1.01[12][d]
21	−2.90788	0.205	8.80049	4.43 [10]	1.43 [−4]	3.70 [−4]	4.5053	1.17 [14]	4.5296	1.51 [12]
22	−3.19820	0.221	9.67616	4.89 [10]	1.46 [−4]	3.39 [−4]	4.9488	1.41 [14]	4.9745	2.32 [12]
			9.674753[b]	2.368[10][b]				1.404[14][b]		2.306[12][b]
							4.9488[d]	1.44[14][d]	4.9746[d]	2.45[12][d]
23	−3.50260	0.239	10.59490	5.36 [10]	1.48 [−4]	3.11 [−4]	5.4140	1.67 [14]	5.4411	3.48 [12]
24	−3.82103	0.259	11.55556	5.85 [10]	1.48 [−4]	2.86 [−4]	5.9003	1.97 [14]	5.9288	5.11 [12]

TABLE II. (*Continued*.)

	Initial state		Final state							
	$(2s2p_{3/2})_1$		$(1s)^2$				$(1s2s)_0$		$(1s2s)_1$	
Z	ΔE (keV)	Γ (eV)	ω (keV)	W (s^{-1})	$\frac{\Gamma_{\rm TEOP}}{\Gamma}$	$\frac{\Gamma_{\rm TEOP}}{\Gamma_{\rm OEOP}}$	ω (keV)	W (s^{-1})	ω (keV)	W (s^{-1})
25	−4.15357	0.283	12.55891	6.36 [10]	1.48 [−4]	2.64 [−4]	6.4081	2.31 [14]	6.4381	7.33 [12]
26	−4.50026	0.309	13.60513	6.88 [10]	1.47 [−4]	2.45 [−4]	6.9375	2.69 [14]	6.9689	1.03 [13]
			13.60968[a]	9.42[10][a]			6.93967[a]	2.78[14][a]		
			13.604082[b]	3.342[10][b]				2.683[14][b]		1.025[13][b]
			13.60475[e]	4.346[10][e]			6.93735[e]	2.636[14][e]	6.96945[e]	1.005[13][e]
							6.9376[d]	2.79[14][d]	6.9690[d]	1.08[13][d]
27	−4.86114	0.338	14.69441	7.42 [10]	1.44 [−4]	2.27 [−4]	7.4887	3.10 [14]	7.5215	1.42 [13]
28	−5.23632	0.371	15.82809	7.98 [10]	1.41 [−4]	2.11 [−4]	8.0623	3.56 [14]	8.0966	1.92 [13]
			15.83249[a]	1.087[11][a]			8.06454[a]	3.71[14][a]		
			15.82642[c]	3.875[10][c]			8.06192[c]	3.561[14][c]	8.09666[c]	1.911[13][c]
			15.82711[e]	5.001[10][e]			8.06175[e]	3.496[14][e]	8.09683[e]	1.881[13][e]
							8.0620[d]	3.72[14][d]	8.0964[d]	2.02[13][d]
29	−5.62570	0.408	17.00424	8.54 [10]	1.38 [−4]	1.96 [−4]	8.6573	4.06 [14]	8.6932	2.56 [13]
			17.00344[e]	5.338[10][e]			8.65688[e]	3.990[14][e]	8.69348[e]	2.505[13][e]
30	−6.02938	0.448	18.22411	9.08 [10]	1.33 [−4]	1.82 [−4]	9.2745	4.60 [14]	9.3119	3.35 [13]
			18.22352[e]	5.682[10][e]			9.27413[e]	4.529[14][e]	9.31228[e]	3.283[13][e]
							9.2745[d]	4.86[14][d]	9.3119[d]	3.52[13][d]
31	−6.44747	0.493	19.48783	9.68 [10]	1.29 [−4]	1.71 [−4]	9.9139	5.20 [14]	9.9528	4.31 [13]
32	−6.87998	0.543	20.79569	1.03 [11]	1.25 [−4]	1.60 [−4]	10.576	5.84 [14]	10.616	5.48 [13]
33	−7.32707	0.597	22.14970	1.09 [11]	1.20 [−4]	1.50 [−4]	11.261	6.53 [14]	11.303	6.87 [13]
34	−7.78861	0.656	23.54681	1.15 [11]	1.16 [−4]	1.41 [−4]	11.968	7.28 [14]	12.012	8.50 [13]
35	−8.26474	0.721	24.98882	1.22 [11]	1.11 [−4]	1.33 [−4]	12.698	8.08 [14]	12.743	1.04 [14]
36	−8.75552	0.792	26.47603	1.29 [11]	1.07 [−4]	1.25 [−4]	13.450	8.94 [14]	13.498	1.26 [14]
			26.47588[e]	7.897[10][e]			13.45021[e]	8.817[14][e]	13.49825[e]	1.245[14][e]
							13.451[d]	9.69[14][d]	13.498[d]	1.35[14][d]
37	−9.26103	0.869	28.00871	1.36 [11]	1.03 [−4]	1.18 [−4]	14.226	9.86 [14]	14.275	1.51 [14]
38	−9.78146	0.952	29.58962	1.43 [11]	9.87 [−5]	1.12 [−4]	15.027	1.09 [15]	15.078	1.80 [14]
39	−10.31663	1.042	31.21442	1.50 [11]	9.47 [−5]	1.06 [−4]	15.850	1.19 [15]	15.902	2.12 [14]
40	−10.86672	1.139	32.88562	1.57 [11]	9.10 [−5]	1.01 [−4]	16.697	1.30 [15]	16.751	2.48 [14]
41	−11.43182	1.244	34.60356	1.65 [11]	8.74 [−5]	9.59 [−5]	17.567	1.42 [15]	17.623	2.87 [14]
			34.60361[e]	1.002[11][e]			17.56701[e]	1.405[15][e]	17.6242[e]	2.884[14][e]
42	−12.01201	1.357	36.36857	1.73 [11]	8.40 [−5]	9.14 [−5]	18.462	1.55 [15]	18.520	3.31 [14]
43	−12.60754	1.478	38.18432	1.81 [11]	8.08 [−5]	8.72 [−5]	19.383	1.68 [15]	19.443	3.79 [14]
44	−13.21816	1.607	40.04492	1.90 [11]	7.77 [−5]	8.34 [−5]	20.326	1.83 [15]	20.388	4.32 [14]
45	−13.84413	1.746	41.95376	1.99 [11]	7.49 [−5]	7.98 [−5]	21.295	1.98 [15]	21.359	4.90 [14]
46	−14.48554	1.894	43.91119	2.08 [11]	7.22 [−5]	7.65 [−5]	22.288	2.14 [15]	22.354	5.52 [14]
47	−15.14247	2.052	45.91768	2.17 [11]	6.96 [−5]	7.35 [−5]	23.307	2.31 [15]	23.375	6.20 [14]
			45.9188[e]	1.313[11][e]			23.30707[e]	2.283[15][e]	23.37657[e]	6.141[14][e]
48	−15.81521	2.220	47.97775	2.26 [11]	6.72 [−5]	7.05 [−5]	24.353	2.49 [15]	24.424	6.93 [14]
49	−16.50353	2.398	50.08396	2.36 [11]	6.49 [−5]	6.79 [−5]	25.423	2.69 [15]	25.496	7.71 [14]
50	−17.20767	2.588	52.24051	2.47 [11]	6.28 [−5]	6.55 [−5]	26.519	2.89 [15]	26.595	8.55 [14]
51	−17.92777	2.788	54.44794	2.58 [11]	6.08 [−5]	6.32 [−5]	27.642	3.10 [15]	27.719	9.45 [14]
52	−18.66392	3.001	56.70665	2.69 [11]	5.89 [−5]	6.11 [−5]	28.791	3.33 [15]	28.871	1.04 [15]
53	−19.41648	3.226	59.02240	2.80 [11]	5.72 [−5]	5.91 [−5]	29.970	3.56 [15]	30.052	1.14 [15]
54	−20.18513	3.463	61.38580	2.92 [11]	5.55 [−5]	5.73 [−5]	31.173	3.81 [15]	31.258	1.25 [15]
55	−20.97021	3.714	63.80221	3.05 [11]	5.40 [−5]	5.55 [−5]	32.404	4.07 [15]	32.491	1.37 [15]
56	−21.77184	3.978	66.27210	3.17 [11]	5.25 [−5]	5.39 [−5]	33.663	4.35 [15]	33.753	1.49 [15]
57	−22.59017	4.255	68.79617	3.31 [11]	5.11 [−5]	5.24 [−5]	34.950	4.64 [15]	35.043	1.62 [15]
58	−23.42554	4.548	71.38098	3.44 [11]	4.98 [−5]	5.10 [−5]	36.269	4.94 [15]	36.364	1.76 [15]
59	−24.27769	4.855	74.01560	3.59 [11]	4.87 [−5]	4.97 [−5]	37.614	5.26 [15]	37.712	1.90 [15]
60	−25.14696	5.177	76.70625	3.74 [11]	4.75 [−5]	4.85 [−5]	38.988	5.59 [15]	39.089	2.06 [15]
61	−26.03350	5.515	79.45333	3.89 [11]	4.64 [−5]	4.73 [−5]	40.392	5.94 [15]	40.496	2.22 [15]
62	−26.93746	5.869	82.25778	4.04 [11]	4.54 [−5]	4.62 [−5]	41.826	6.30 [15]	41.933	2.39 [15]
63	−27.85929	6.239	85.12839	4.21 [11]	4.44 [−5]	4.51 [−5]	43.294	6.69 [15]	43.405	2.57 [15]

TABLE II. (*Continued.*)

	Initial state		Final state							
	$(2s2p_{3/2})_1$		$(1s)^2$				$(1s2s)_0$		$(1s2s)_1$	
Z	ΔE (keV)	Γ (eV)	ω (keV)	W (s^{-1})	$\frac{\Gamma_{\rm TEOP}}{\Gamma}$	$\frac{\Gamma_{\rm TEOP}}{\Gamma_{\rm OEOP}}$	ω (keV)	W (s^{-1})	ω (keV)	W (s^{-1})
64	−28.79860	6.627	88.04973	4.38 [11]	4.35 [−5]	4.42 [−5]	44.790	7.08 [15]	44.904	2.75 [15]
65	−29.75602	7.032	91.03262	4.55 [11]	4.26 [−5]	4.32 [−5]	46.318	7.50 [15]	46.435	2.95 [15]
66	−30.73142	7.454	94.07422	4.73 [11]	4.18 [−5]	4.24 [−5]	47.877	7.93 [15]	47.997	3.15 [15]
67	−31.72527	7.896	97.17853	4.92 [11]	4.10 [−5]	4.15 [−5]	49.469	8.38 [15]	49.593	3.37 [15]
68	−32.73767	8.356	100.35217	5.11 [11]	4.02 [−5]	4.08 [−5]	51.098	8.85 [15]	51.226	3.59 [15]
69	−33.76881	8.835	103.58261	5.31 [11]	3.95 [−5]	4.00 [−5]	52.758	9.34 [15]	52.889	3.82 [15]
70	−34.81879	9.334	106.87600	5.51 [11]	3.89 [−5]	3.93 [−5]	54.450	9.84 [15]	54.585	4.07 [15]
71	−35.88801	9.853	110.23530	5.72 [11]	3.82 [−5]	3.87 [−5]	56.178	1.04 [16]	56.317	4.32 [15]
72	−36.97664	10.393	113.66090	5.94 [11]	3.76 [−5]	3.80 [−5]	57.942	1.09 [16]	58.084	4.59 [15]
73	−38.08481	10.954	117.16167	6.17 [11]	3.71 [−5]	3.74 [−5]	59.745	1.15 [16]	59.892	4.86 [15]
74	−39.21296	11.536	120.72321	6.40 [11]	3.65 [−5]	3.69 [−5]	61.581	1.21 [16]	61.732	5.15 [15]
75	−40.36134	12.141	124.35508	6.65 [11]	3.60 [−5]	3.64 [−5]	63.455	1.27 [16]	63.610	5.45 [15]
76	−41.53000	12.767	128.05628	6.90 [11]	3.55 [−5]	3.59 [−5]	65.366	1.33 [16]	65.526	5.76 [15]
77	−42.71947	13.417	131.83066	7.16 [11]	3.51 [−5]	3.54 [−5]	67.317	1.40 [16]	67.481	6.08 [15]
78	−43.92943	14.090	135.68517	7.42 [11]	3.47 [−5]	3.49 [−5]	69.310	1.46 [16]	69.479	6.42 [15]
79	−45.16112	14.786	139.60759	7.70 [11]	3.43 [−5]	3.45 [−5]	71.341	1.53 [16]	71.515	6.76 [15]
80	−46.41437	15.507	143.60552	7.98 [11]	3.39 [−5]	3.41 [−5]	73.412	1.61 [16]	73.591	7.12 [15]
81	−47.68958	16.252	147.68134	8.27 [11]	3.35 [−5]	3.37 [−5]	75.526	1.68 [16]	75.710	7.49 [15]
82	−48.98695	17.023	151.83613	8.55 [11]	3.31 [−5]	3.33 [−5]	77.683	1.76 [16]	77.872	7.88 [15]
83	−50.30608	17.818	156.07752	8.86 [11]	3.27 [−5]	3.29 [−5]	79.886	1.84 [16]	80.081	8.27 [15]
84	−51.64925	18.640	160.39672	9.19 [11]	3.24 [−5]	3.26 [−5]	82.132	1.92 [16]	82.333	8.68 [15]
85	−53.01553	19.488	164.79712	9.52 [11]	3.21 [−5]	3.23 [−5]	84.423	2.00 [16]	84.630	9.11 [15]
86	−54.40594	20.362	169.28698	9.86 [11]	3.19 [−5]	3.20 [−5]	86.763	2.09 [16]	86.975	9.55 [15]
87	−55.82048	21.264	173.86368	1.02 [12]	3.16 [−5]	3.18 [−5]	89.150	2.18 [16]	89.369	10.0 [15]
88	−57.25791	22.193	178.53350	1.06 [12]	3.14 [−5]	3.15 [−5]	91.588	2.27 [16]	91.813	1.05 [16]
89	−58.72168	23.150	183.28747	1.09 [12]	3.11 [−5]	3.13 [−5]	94.073	2.36 [16]	94.305	1.09 [16]
90	−60.21096	24.135	188.13466	1.13 [12]	3.09 [−5]	3.10 [−5]	96.610	2.46 [16]	96.848	1.14 [16]
91	−61.72624	25.148	193.07718	1.17 [12]	3.07 [−5]	3.08 [−5]	99.199	2.56 [16]	99.445	1.19 [16]
92	−63.26803	26.191	198.11731	1.21 [12]	3.05 [−5]	3.06 [−5]	101.84	2.66 [16]	102.10	1.25 [16]

are $\leqslant$4.3% for the E2 transitions. For neon ion, the relative differences are $\leqslant$11% and $\leqslant$8.7% for the E1 transitions from the $(2s2p_{3/2})_1$ and $(2s2p_{1/2})_1$ states, respectively, and are $\leqslant$34% for the E2 transitions. For the E2 transitions in boron ion, the relative difference is so large that we conclude that the perturbation theory does not work (it also manifests itself in a significant difference between W_0 and W). However, the results for the E1 transitions in boron are still plausible: the relative differences are $\leqslant$16% and $\leqslant$7% for $(2s2p_{3/2})_1$ and $(2s2p_{1/2})_1$, respectively.

A feature of the TEOP transitions is that both electrons of the initial states change their quantum numbers. Hence, the TEOP transitions proceed due to the interelectron interaction. The necessity of this interaction makes such transitions considerably weaker than those which can be described without interelectron interaction. Below, we focus our attention on the TEOP $(2s2p)_1 \to (1s)^2$ transitions which are characterized by the highest branching ratios.

In Tables II and III, we present the TEOP transition probabilities for the $(2s2p_{1/2})_1$ $^3P_1$ and $(2s2p_{3/2})_1$ $^1P_1$ states, respectively, to the ground states $(1s)^2$ $^1S_0$ of the He-like sequence of atomic ions. In order to compare the TEOP and OEOP transitions, the transition probabilities to the $(1s2s)_0$ $^1S_0$ and $(1s2s)_1$ $^3S_1$ single excited states are also presented. We note that for the $(2s2p_{1/2})_1$ $^3P_1$ state, the transitions to the $(1s2s)_1$ $^3S_1$ state are the main radiative decay channel, while the transitions to the $(1s)^2$, $(1s2s)_0$ $^1S_0$ state are spin forbidden in the nonrelativistic limit. For the case of the $(2s2p_{3/2})_1$ $^1P_1$ state, the situation is reversed: the transitions to the $(1s2s)_0$ $^1S_0$ state are the main decay channel and the transitions to the $(1s2s)_1$ $^3S_1$ state are spin forbidden in the nonrelativistic limit. Accordingly, the TEOP transition $(2s2p_{1/2})_1$ $^3P_1 \to$ $(1s)^2$ $^1S_0$ has an additional smallness compared to the TEOP transition $(2s2p_{3/2})_1$ $^1P_1 \to$ $(1s)^2$ $^1S_0$ in the region of small Z. In Fig. 2, we present the TEOP transition probabilities W as a function of Z. In the case of the spin-allowed $(2s2p_{3/2})_1$ $^1P_1 \to$ $(1s)^2$ $^1S_0$ transition, the dependence of W on Z is rather simple: $W \sim Z^2$ [4]. For heavy ions, relativistic effects lead to a deviation of the Z^2 dependence. For the spin-forbidden $(2s2p_{1/2})_1$ $^3P_1 \to$ $(1s)^2$ $^1S_0$ transition, the dependence on Z is not power law.

In Fig. 3, we present the relative difference $|W^{(\rm L)} - W^{(\rm V)}|/W^{(\rm L)}$ between the values of the transition probabilities calculated in the velocity and length gauges as a function of Z. This relative difference can be used for estimation of the

TABLE III. The same as in Table II, but for the $(2s2p_{1/2})_1$ state.

	Initial state		Final state							
	$(2s2p_{1/2})_1$		$(1s)^2$				$(1s2s)_0$		$(1s2s)_1$	
Z	ΔE (keV)	Γ (eV)	ω (keV)	W (s^{-1})	$\frac{\Gamma_{\rm TEOP}}{\Gamma}$	$\frac{\Gamma_{\rm TEOP}}{\Gamma_{\rm OEOP}}$	ω (keV)	W (s^{-1})	ω (keV)	W (s^{-1})
5	−0.15275	0.008	0.44666	1.20 [4]	9.72 [−10]	3.29 [−8]	0.24384	1.48 [6]	0.24821	3.26 [11]
			0.446197[b]	7.110[3][b]				1.358[6][b]		3.284[11][b]
6	−0.22404	0.009	0.65790	4.55 [4]	3.45 [−9]	5.93 [−8]	0.35351	8.40 [6]	0.35904	6.99 [11]
			0.657394[b]	2.276[4][b]				8.148[6][b]		7.020[11][b]
							0.35363[d]	7.66[6][d]	0.35905[d]	7.11[11][d]
7	−0.30896	0.009	0.91003	1.44 [5]	1.01 [−8]	1.01 [−7]	0.48362	3.77 [7]	0.49033	1.32 [12]
			0.909475[b]	9.158[4][b]				3.724[7][b]		1.330[12][b]
							0.48372[d]	3.48[7][d]	0.49033[d]	1.34[12][d]
8	−0.40755	0.010	1.20308	3.99 [5]	2.57 [−8]	1.62 [−7]	0.63420	1.38 [8]	0.64210	2.30 [12]
			1.202496[b]	2.497[5][b]				1.385[8][b]		2.304[12][b]
							0.63428[d]	1.29[8][d]	0.64210[d]	2.32[12][d]
9	−0.51981	0.011	1.53711	9.98 [5]	5.75 [−8]	2.52 [−7]	0.80527	4.42 [8]	0.81437	3.73 [12]
			1.536491[b]	6.060[5][b]				4.417[8][b]		3.736[12][b]
							0.80533[d]	4.13[8][d]	0.81437[d]	3.77[12][d]
10	−0.64577	0.013	1.91214	2.28 [6]	1.15 [−7]	3.77 [−7]	0.99686	1.25 [9]	1.0072	5.74 [12]
			1.911507[b]	1.343[6][b]				1.246[9][b]		5.751[12][b]
			1.91125[e]	1.648[6][e]			0.99638[e]	1.042[9][e]	1.00722[e]	5.661[12][e]
							0.99692[d]	1.17[9][d]	1.0072[d]	5.80[12][d]
11	−0.78544	0.015	2.32825	4.78 [6]	2.08 [−7]	5.37 [−7]	1.2090	3.19 [9]	1.2205	8.48 [12]
12	−0.93886	0.018	2.78547	9.44 [6]	3.49 [−7]	7.47 [−7]	1.4417	7.50 [9]	1.4545	1.21 [13]
			2.784820[b]	5.332[6][b]				7.471[9][b]		1.210[13][b]
							1.4418[d]	7.03[9][d]	1.4545[d]	1.22[13][d]
13	−1.10606	0.021	3.28403	1.76 [7]	5.45 [−7]	1.01 [−6]	1.6951	1.64 [10]	1.7091	1.67 [13]
14	−1.28705	0.026	3.82373	3.12 [7]	8.06 [−7]	1.33 [−6]	1.9691	3.39 [10]	1.9844	2.26 [13]
			3.822746[b]	1.715[7][b]				3.375[10][b]		2.262[13][b]
			3.82279[e]	1.955[7][e]			1.96859[e]	3.090[10][e]	1.98441[e]	2.239[13][e]
							1.9691[d]	3.19[10][d]	1.9844[d]	2.28[13][d]
15	−1.48188	0.031	4.40477	5.33 [7]	1.14 [−6]	1.72 [−6]	2.2638	6.64 [10]	2.2803	2.99 [13]
16	−1.69058	0.037	5.02723	8.76 [7]	1.55 [−6]	2.18 [−6]	2.5792	1.24 [11]	2.5970	3.88 [13]
17	−1.91320	0.045	5.69119	1.39 [8]	2.04 [−6]	2.71 [−6]	2.9154	2.22 [11]	2.9345	4.96 [13]
18	−2.14979	0.054	6.39711	2.15 [8]	2.62 [−6]	3.33 [−6]	3.2727	3.84 [11]	3.2931	6.24 [13]
			6.396059[b]	1.138[8][b]				3.818[11][b]		6.238[13][b]
			6.39607[e]	1.307[8][e]			3.27206[e]	3.611[11][e]	3.29305[e]	6.179[13][e]
							3.2726[d]	3.63[11][d]	3.2930[d]	6.33[13][d]
19	−2.40037	0.065	7.14444	3.24 [8]	3.28 [−6]	4.03 [−6]	3.6506	6.42 [11]	3.6723	7.75 [13]
20	−2.66500	0.078	7.93358	4.75 [8]	4.03 [−6]	4.82 [−6]	4.0495	1.04 [12]	4.0726	9.51 [13]
			7.933026[b]	2.491[8][b]				1.034[12][b]		9.509[13][b]
			7.93267[e]	2.860[8][e]			4.04897[e]	9.8669[11][e]	4.07263[e]	9.432[13][e]
							4.0495[d]	9.86[11][d]	4.0726[d]	9.67[13][d]
21	−2.94373	0.092	8.76464	6.82 [8]	4.85 [−6]	5.68 [−6]	4.4694	1.64 [12]	4.4938	1.15 [14]
22	−3.23663	0.110	9.63773	9.57 [8]	5.75 [−6]	6.61 [−6]	4.9104	2.51 [12]	4.9361	1.39 [14]
			9.635396[b]	4.986[8][b]				2.500[12][b]		1.388[14][b]
							4.9105[d]	2.39[12][d]	4.9363[d]	1.42[14][d]
23	−3.54380	0.129	10.55369	1.32 [9]	6.72 [−6]	7.61 [−6]	5.3728	3.76 [12]	5.3999	1.65 [14]
24	−3.86523	0.151	11.51136	1.78 [9]	7.74 [−6]	8.66 [−6]	5.8561	5.51 [12]	5.8846	1.95 [14]
25	−4.20102	0.176	12.51146	2.36 [9]	8.81 [−6]	9.76 [−6]	6.3606	7.88 [12]	6.3906	2.29 [14]
26	−4.55125	0.205	13.55414	3.08 [9]	9.90 [−6]	1.09 [−5]	6.8865	1.11 [13]	6.9179	2.67 [14]
			13.553011[b]	1.599[9][b]				1.100[13][b]		2.666[14][b]
			13.55346[e]	1.828[9][e]			6.88605[e]	1.067[13][e]	6.91815[e]	2.655[14][e]
							6.8867[d]	1.06[13][d]	6.9181[d]	2.74[14][d]
27	−4.91599	0.237	14.63955	3.96 [9]	1.10 [−5]	1.20 [−5]	7.4338	1.52 [13]	7.4667	3.08 [14]
28	−5.29539	0.272	15.76902	5.01 [9]	1.21 [−5]	1.31 [−5]	8.0032	2.06 [13]	8.0375	3.54 [14]
			15.76805[c]	2.607[9][c]			8.00259[c]	2.051[13][c]	8.03735[c]	3.537[14][c]
			15.76773[e]	2.955[9][e]			8.00238[e]	1.992[13][e]	8.03745[e]	3.576[14][e]
							8.0031[d]	1.97[13][d]	8.0374[d]	3.66[14][d]

TABLE III. (*Continued.*)

	Initial state		Final state							
	$(2s2p_{1/2})_1$		$(1s)^2$				$(1s2s)_0$		$(1s2s)_1$	
Z	ΔE (keV)	Γ (eV)	ω (keV)	W (s^{-1})	$\frac{\Gamma_{\rm TEOP}}{\Gamma}$	$\frac{\Gamma_{\rm TEOP}}{\Gamma_{\rm OEOP}}$	ω (keV)	W (s^{-1})	ω (keV)	W (s^{-1})
29	−5.68942	0.312	16.94052	6.26 [9]	1.32 [−5]	1.42 [−5]	8.5936	2.73 [13]	8.6295	4.05 [14]
			16.93945[e]	3.676[9][e]			8.59288[e]	2.652[13][e]	8.62948[e]	4.029[14][e]
30	−6.09821	0.356	18.15527	7.75 [9]	1.43 [−5]	1.54 [−5]	9.2057	3.57 [13]	9.2431	4.60 [14]
			18.15446[e]	4.512[9][e]			9.20507[e]	3.472[13][e]	9.24322[e]	4.578[14][e]
							9.2058[d]	3.43[13][d]	9.2432[d]	4.77[14][d]
31	−6.52187	0.404	19.41343	9.42 [9]	1.53 [−5]	1.64 [−5]	9.8395	4.60 [13]	9.8784	5.20 [14]
32	−6.96048	0.457	20.71519	1.13 [10]	1.63 [−5]	1.73 [−5]	10.495	5.84 [13]	10.536	5.85 [14]
33	−7.41424	0.516	22.06253	1.33 [10]	1.70 [−5]	1.80 [−5]	11.174	7.32 [13]	11.216	6.55 [14]
34	−7.88309	0.580	23.45232	1.56 [10]	1.78 [−5]	1.88 [−5]	11.873	9.06 [13]	11.917	7.31 [14]
35	−8.36721	0.649	24.88635	1.82 [10]	1.85 [−5]	1.95 [−5]	12.595	1.11 [14]	12.641	8.13 [14]
36	−8.86672	0.725	26.36484	2.11 [10]	1.91 [−5]	2.01 [−5]	13.339	1.34 [14]	13.386	9.01 [14]
			26.3645[e]	1.220[10][e]			13.33882[e]	1.318[14][e]	13.38687[e]	8.977[14][e]
							13.340[d]	1.31[14][d]	13.387[d]	9.49[14][d]
37	−9.38172	0.808	27.88802	2.42 [10]	1.97 [−5]	2.06 [−5]	14.106	1.61 [14]	14.155	9.95 [14]
38	−9.91248	0.897	29.45860	2.76 [10]	2.02 [−5]	2.11 [−5]	14.896	1.91 [14]	14.947	1.10 [15]
39	−10.45887	0.994	31.07217	3.11 [10]	2.06 [−5]	2.15 [−5]	15.708	2.26 [14]	15.760	1.21 [15]
40	−11.02113	1.098	32.73121	3.50 [10]	2.10 [−5]	2.18 [−5]	16.542	2.64 [14]	16.597	1.32 [15]
41	−11.59940	1.211	34.43598	3.92 [10]	2.13 [−5]	2.21 [−5]	17.400	3.06 [14]	17.456	1.45 [15]
			34.43588[e]	2.232[10][e]			17.39928[e]	3.013[14][e]	17.45647[e]	1.440[15][e]
42	−12.19382	1.332	36.18676	4.35 [10]	2.15 [−5]	2.23 [−5]	18.280	3.53 [14]	18.338	1.58 [15]
43	−12.80469	1.461	37.98717	4.82 [10]	2.17 [−5]	2.24 [−5]	19.185	4.05 [14]	19.246	1.72 [15]
44	−13.43186	1.601	39.83123	5.31 [10]	2.18 [−5]	2.25 [−5]	20.113	4.62 [14]	20.175	1.87 [15]
45	−14.07562	1.750	41.72227	5.83 [10]	2.19 [−5]	2.26 [−5]	21.063	5.24 [14]	21.127	2.03 [15]
46	−14.73614	1.909	43.66059	6.37 [10]	2.20 [−5]	2.26 [−5]	22.038	5.91 [14]	22.104	2.20 [15]
47	−15.41358	2.080	45.64658	6.94 [10]	2.20 [−5]	2.25 [−5]	23.036	6.64 [14]	23.104	2.38 [15]
			45.6476[e]	3.917[10][e]			23.03686[e]	6.548[14][e]	23.10536[e]	2.371[15][e]
48	−16.10828	2.261	47.68469	7.53 [10]	2.19 [−5]	2.25 [−5]	24.060	7.43 [14]	24.131	2.57 [15]
49	−16.82010	2.454	49.76739	8.16 [10]	2.19 [−5]	2.24 [−5]	25.107	8.28 [14]	25.180	2.77 [15]
50	−17.54937	2.660	51.89881	8.81 [10]	2.18 [−5]	2.23 [−5]	26.178	9.20 [14]	26.253	2.99 [15]
51	−18.29630	2.879	54.07941	9.50 [10]	2.17 [−5]	2.22 [−5]	27.273	1.02 [15]	27.351	3.22 [15]
52	−19.06107	3.111	56.30950	1.02 [11]	2.16 [−5]	2.21 [−5]	28.394	1.12 [15]	28.474	3.46 [15]
53	−19.84407	3.357	58.59481	1.10 [11]	2.15 [−5]	2.19 [−5]	29.542	1.24 [15]	29.624	3.71 [15]
54	−20.64518	3.617	60.92575	1.17 [11]	2.14 [−5]	2.18 [−5]	30.713	1.36 [15]	30.798	3.98 [15]
55	−21.46477	3.893	63.30764	1.26 [11]	2.12 [−5]	2.16 [−5]	31.909	1.48 [15]	31.997	4.27 [15]
56	−22.30308	4.184	65.74086	1.34 [11]	2.11 [−5]	2.14 [−5]	33.132	1.62 [15]	33.222	4.57 [15]
57	−23.16034	4.492	68.22600	1.43 [11]	2.09 [−5]	2.13 [−5]	34.380	1.76 [15]	34.472	4.88 [15]
58	−24.03695	4.816	70.76956	1.52 [11]	2.08 [−5]	2.11 [−5]	35.657	1.92 [15]	35.753	5.22 [15]
59	−24.93289	5.158	73.36040	1.61 [11]	2.06 [−5]	2.09 [−5]	36.958	2.08 [15]	37.057	5.57 [15]
60	−25.84854	5.519	76.00467	1.71 [11]	2.04 [−5]	2.07 [−5]	38.286	2.25 [15]	38.387	5.94 [15]
61	−26.78417	5.898	78.70265	1.82 [11]	2.03 [−5]	2.05 [−5]	39.641	2.43 [15]	39.745	6.32 [15]
62	−27.74008	6.297	81.45517	1.92 [11]	2.01 [−5]	2.04 [−5]	41.023	2.62 [15]	41.130	6.73 [15]
63	−28.71672	6.716	84.27097	2.03 [11]	1.99 [−5]	2.02 [−5]	42.437	2.82 [15]	42.547	7.16 [15]
64	−29.71403	7.156	87.13430	2.15 [11]	1.98 [−5]	2.00 [−5]	43.874	3.03 [15]	43.988	7.60 [15]
65	−30.73272	7.618	90.05592	2.27 [11]	1.96 [−5]	1.98 [−5]	45.341	3.25 [15]	45.458	8.07 [15]
66	−31.77277	8.102	93.03287	2.39 [11]	1.94 [−5]	1.97 [−5]	46.836	3.49 [15]	46.956	8.56 [15]
67	−32.83483	8.610	96.06897	2.52 [11]	1.93 [−5]	1.95 [−5]	48.360	3.73 [15]	48.484	9.08 [15]
68	−33.91897	9.141	99.17087	2.65 [11]	1.91 [−5]	1.93 [−5]	49.917	3.99 [15]	50.044	9.61 [15]
69	−35.02589	9.697	102.32552	2.79 [11]	1.89 [−5]	1.92 [−5]	51.501	4.26 [15]	51.632	1.02 [16]
70	−36.15570	10.279	105.53909	2.93 [11]	1.88 [−5]	1.90 [−5]	53.113	4.54 [15]	53.248	1.08 [16]
71	−37.30899	10.887	108.81432	3.08 [11]	1.86 [−5]	1.88 [−5]	54.757	4.84 [15]	54.896	1.14 [16]
72	−38.48610	11.522	112.15144	3.24 [11]	1.85 [−5]	1.87 [−5]	56.432	5.15 [15]	56.575	1.20 [16]
73	−39.68709	12.186	115.55939	3.39 [11]	1.83 [−5]	1.85 [−5]	58.143	5.47 [15]	58.289	1.27 [16]
74	−40.91315	12.878	119.02302	3.56 [11]	1.82 [−5]	1.84 [−5]	59.881	5.81 [15]	60.032	1.34 [16]
75	−42.16447	13.599	122.55194	3.73 [11]	1.80 [−5]	1.82 [−5]	61.652	6.16 [15]	61.807	1.41 [16]
76	−43.44134	14.351	126.14494	3.90 [11]	1.79 [−5]	1.80 [−5]	63.455	6.53 [15]	63.615	1.49 [16]

TABLE III. (*Continued*.)

	Initial state		Final state							
	$(2s2p_{1/2})_1$		$(1s)^2$				$(1s2s)_0$		$(1s2s)_1$	
Z	ΔE (keV)	Γ (eV)	ω (keV)	W (s^{-1})	$\frac{\Gamma_{TEOP}}{\Gamma}$	$\frac{\Gamma_{TEOP}}{\Gamma_{OEOP}}$	ω (keV)	W (s^{-1})	ω (keV)	W (s^{-1})
77	−44.74452	15.135	129.80560	4.08 [11]	1.77 [−5]	1.79 [−5]	65.292	6.92 [15]	65.456	1.56 [16]
78	−46.07349	15.952	133.54111	4.26 [11]	1.76 [−5]	1.78 [−5]	67.166	7.32 [15]	67.335	1.65 [16]
79	−47.43063	16.802	137.33808	4.46 [11]	1.75 [−5]	1.76 [−5]	69.071	7.73 [15]	69.245	1.73 [16]
80	−48.81559	17.686	141.20430	4.65 [11]	1.73 [−5]	1.75 [−5]	71.011	8.17 [15]	71.190	1.82 [16]
81	−50.22907	18.605	145.14184	4.86 [11]	1.72 [−5]	1.73 [−5]	72.986	8.62 [15]	73.171	1.91 [16]
82	−51.67167	19.560	149.15141	5.06 [11]	1.70 [−5]	1.72 [−5]	74.998	9.09 [15]	75.188	2.01 [16]
83	−53.14238	20.554	153.24123	5.28 [11]	1.69 [−5]	1.70 [−5]	77.050	9.58 [15]	77.245	2.11 [16]
84	−54.64531	21.585	157.40066	5.50 [11]	1.68 [−5]	1.69 [−5]	79.136	1.01 [16]	79.337	2.21 [16]
85	−56.17917	22.655	161.63348	5.73 [11]	1.66 [−5]	1.68 [−5]	81.259	1.06 [16]	81.466	2.32 [16]
86	−57.74541	23.766	165.94752	5.96 [11]	1.65 [−5]	1.66 [−5]	83.423	1.12 [16]	83.636	2.43 [16]
87	−59.34434	24.919	170.33982	6.20 [11]	1.64 [−5]	1.65 [−5]	85.626	1.17 [16]	85.845	2.54 [16]
88	−60.97402	26.115	174.81739	6.44 [11]	1.62 [−5]	1.64 [−5]	87.872	1.23 [16]	88.097	2.66 [16]
89	−62.64049	27.353	179.36866	6.69 [11]	1.61 [−5]	1.62 [−5]	90.154	1.29 [16]	90.386	2.78 [16]
90	−64.34231	28.636	184.00331	6.95 [11]	1.60 [−5]	1.61 [−5]	92.478	1.35 [16]	92.717	2.91 [16]
91	−66.08031	29.965	188.72311	7.19 [11]	1.58 [−5]	1.59 [−5]	94.845	1.42 [16]	95.091	3.04 [16]
92	−67.85577	31.341	193.52957	7.45 [11]	1.57 [−5]	1.58 [−5]	97.254	1.49 [16]	97.507	3.18 [16]

calculation accuracy. In general, the accuracy of the OEOP transitions is better than the accuracy for TEOP transitions. The gauge invariance for the TEOP transitions was investigated in works [5,7]. In work [5], it was 26% for $Z = 4$ and 35% for $Z = 26$, and in work [7], it was 20–50% for $Z = 10$–47.

The branching ratio Γ_{TEOP}/Γ and the intensity ratio $\Gamma_{TEOP}/\Gamma_{OEOP}$ can provide valuable information to experimentally study the TEOP transitions. In Fig. 4, we present these ratios as a function of Z. It shows that the branching ratio Γ_{TEOP}/Γ has nonmonotonic behavior. This can be explained as follows: (a) Γ_{TEOP} increases with Z; (b) Γ has near-constant behavior for small Z ($\Gamma \approx \Gamma_{Auger}$, where Γ_{Auger} denotes the Auger width) and $\Gamma \sim Z^4$ for large Z ($\Gamma \approx \Gamma_{rad}$, where Γ_{rad} denotes the radiative width).

The intensity ratio $\Gamma_{TEOP}/\Gamma_{OEOP}$ is measurable and presents a comparison of the TEOP and OEOP transitions. Unlike the total width Γ, Γ_{OEOP} does not contain the Γ_{Auger} and Γ_{TEOP} widths ($\Gamma_{OEOP} = \Gamma - \Gamma_{Auger} - \Gamma_{TEOP} \approx \Gamma_{rad}$). Due to the simplicity of the Z dependence of Γ_{TEOP} for the $(2s2p_{3/2})_1$ $^1P_1$ state, the ratio shows monotonic behavior ($\sim Z^{-2}$). For the $(2s2p_{1/2})_1$ $^3P_1$ state, the ratio has a similar behavior for large Z, while for small Z, it is more complicated

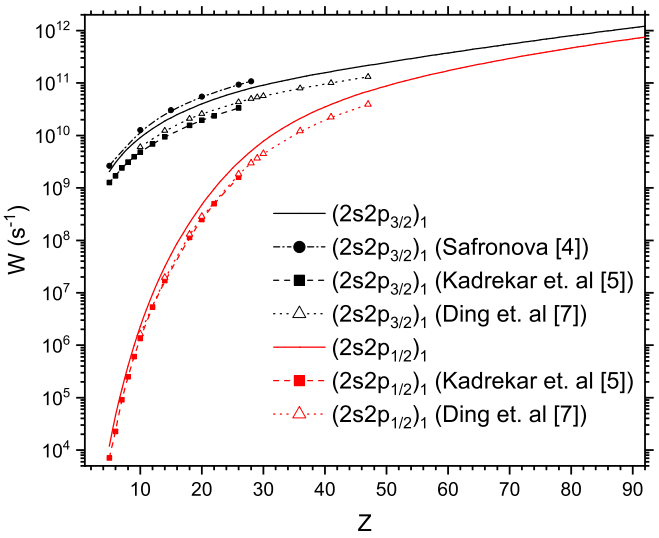

FIG. 2. Transition probabilities (W) as functions of Z for $(2s2p_{3/2})_1$ $^1P_1 \rightarrow$ $(1s)^2$ $^1S_0$ (black curves) and $(2s2p_{1/2})_1$ $^3P_1 \rightarrow$ $(1s)^2$ $^1S_0$ (red curves) transitions. The results of [5,7] are presented in the length gauge; the results of [4] are presented in the dipole approximation. The difference between our results obtained in different gauges is barely noticeable in the scale of this plot.

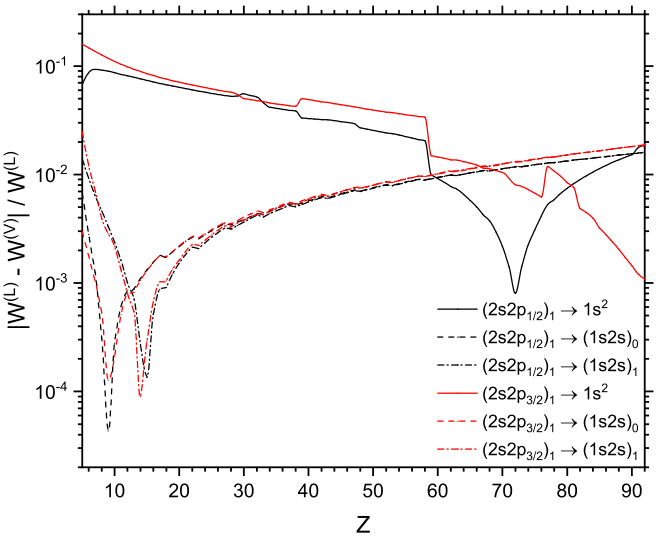

FIG. 3. Relative difference ($|W^{(L)} - W^{(V)}|/W^{(L)}$) between the values of the transition probabilities calculated in the velocity and length gauges as a function of Z.

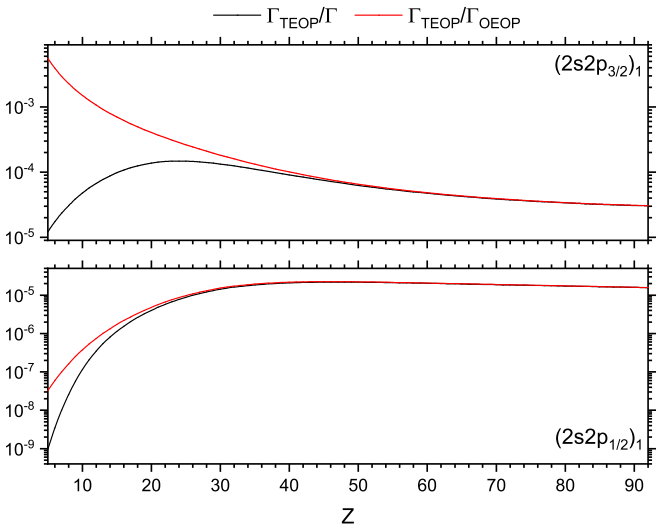

FIG. 4. Branching ratio $\Gamma_{\mathrm{TEOP}}/\Gamma$ (black curves) and intensity ratio $\Gamma_{\mathrm{TEOP}}/\Gamma_{\mathrm{OEOP}} = W_{\mathrm{TEOP}}/W_{\mathrm{OEOP}}$ (red curves) for $(2s2p_{3/2})_1\ {}^1P_1 \to (1s)^2\ {}^1S_0$ (upper panel) and $(2s2p_{1/2})_1\ {}^3P_1 \to (1s)^2\ {}^1S_0$ (lower panel) transitions as functions of Z.

since the corresponding TEOP transition is spin forbidden in the nonrelativistic limit.

In Tables II and III, we compare our results with results of other works [4–8]. A reasonable agreement was found with the work of Safronova [4], where the dipole approximation and the perturbation theory for the electron-electron interaction were used. The reason for the discrepancy is that our work goes beyond the dipole approximation and takes into account the second order (and partly higher orders) in the interelectron interaction and the radiative corrections.

We also compare our results with those obtained using the GRASP code [13,14]: Kadrekar and Natarajan [5,6] and Ding *et al.* [7]. The difference in the results significantly exceeds the accuracy of our calculation, which is estimated as the difference between the results in the velocity and length gauges. Our results for the TEOP transition probabilities are roughly two times larger than the results of [5,6].

In Tables II and III, we also provide a comparison of our results for OEOP transition probabilities and transition energies with other authors. The results are in good agreement.

IV. SUMMARY

We investigated TEOP $(2s2p)_1 \to (1s)^2$ transitions for the He-like sequence of atomic ions. The corresponding transition probabilities and transition energies were calculated within the QED theory. The one- and two-photon exchange corrections were taken into account as well as the electron self-energy and vacuum polarization corrections. The gauge invariance of the obtained results was investigated. In the case of low- and middle-Z ions, it was found that the violation of the gauge invariance for TEOP transitions is 1–3 orders of magnitude larger than the one for OEOP transitions. Due to the strong degeneracy of the autoionizing states, the TEOP transitions are much more sensitive to the interelectron interaction. Taking into account the higher-order interelectron interaction corrections, in particular, the exact treatment of the electron self-energy and vacuum polarization screening corrections should improve the gauge invariance. The intensity ratios between the TEOP transitions and the other major transitions were presented. These ratios can be measured in future experiments. For the study of TEOP transitions, an important issue is the formation of autoionizing states. One of the most promising ways is to observe the TEOP transitions in the process of dielectronic recombination [28]. In this case, autoionization states can decay along several channels. The branching ratios are necessary for compiling a complete picture of the decay of the autoionization state.

ACKNOWLEDGMENTS

We are grateful to Professor Jacek Rzadkiewicz and Professor Karol Kozioł for reading the manuscript. This work is supported by the National Key Research and Development Program of China under Grant No. 2017YFA0402300, the Chinese Postdoctoral Science Foundation Grant No. 2020M673538, the National Natural Science Foundation of China under Grant No. 11774356, and the Chinese Academy of Sciences (CAS) Presidents International Fellowship Initiative (PIFI) under Grant No. 2018VMB0016. The reported study was funded by RFBR and NSFC according to the research Project No. 20-52-53028. The work of O.Y.A. on the calculation of the differential transition probabilities was supported solely by the Russian Science Foundation under Grant No. 17-12-01035.

[1] K. N. Lyashchenko and O. Y. Andreev, Phys. Rev. A **98**, 012503 (2018).
[2] K. N. Lyashchenko, O. Y. Andreev, and A. B. Voitkiv, Phys. Rev. A **96**, 052702 (2017).
[3] K. J. LaGattuta and Y. Hahn, Phys. Rev. A **24**, 2273 (1981).
[4] U. I. Safronova and V. S. Senashenko, J. Phys. B **10**, L271 (1977).
[5] R. Kadrekar and L. Natarajan, Phys. Rev. A **84**, 062506 (2011).
[6] L. Natarajan and R. Kadrekar, Phys. Rev. A **88**, 012501 (2013).
[7] X. Ding, C. Wu, M. Cao, D. Zhang, M. Zhang, Y. Xue, D. Yu, and C. Dong, Chin. Phys. B **29**, 033101 (2020).
[8] F. Goryaev, L. Vainshtein, and A. Urnov, At. Data Nucl. Data Tables **113**, 117 (2017).
[9] D. Zhang, C. Dong, and K. Fumihiro, Chin. Phys. Lett. **23**, 2059 (2006).
[10] L. Natarajan, Phys. Rev. A **90**, 032509 (2014).
[11] V. Shevelko and L. Vainshtein, *Atomic Physics for Hot Plasmas* (Institute of Physics Publishing, Bristol, 1993).
[12] L. Vainshtein and U. Safronova, At. Data Nucl. Data Tables **21**, 49 (1978).
[13] F. Parpia, C. Fischer, and I. Grant, Comput. Phys. Commun. **94**, 249 (1996).
[14] P. Jönsson, X. He, C. F. Fischer, and I. Grant, Comput. Phys. Commun. **177**, 597 (2007).
[15] W. Wölfli, C. Stoller, G. Bonani, M. Suter, and M. Stöckli, Phys. Rev. Lett. **35**, 656 (1975).

[16] R. Elton, J. Cobble, H. Griem, D. Montgomery, R. Mancini, V. Jacobs, and E. Behar, J. Quantum Spectrosc. Radiat. Transfer **65**, 185 (2000).

[17] F. B. Rosmej, H. R. Griem, R. C. Elton, V. L. Jacobs, J. A. Cobble, A. Y. Faenov, T. A. Pikuz, M. Geißel, D. H. H. Hoffmann, W. Süß, D. B. Uskov, V. P. Shevelko, and R. C. Mancini, Phys. Rev. E **66**, 056402 (2002).

[18] Y. Zou, J. R. Crespo López-Urrutia, and J. Ullrich, Phys. Rev. A **67**, 042703 (2003).

[19] M. Togawa, S. Kühn, C. Shah, P. Amaro, R. Steinbrügge, J. Stierhof, N. Hell, M. Rosner, K. Fujii, M. Bissinger, R. Ballhausen, M. Hoesch, J. Seltmann, S. Park, F. Grilo, F. S. Porter, J. P. Santos, M. Chung, T. Stöhlker, J. Wilms *et al.*, Phys. Rev. A **102**, 052831 (2020).

[20] O. Yu. Andreev, L. N. Labzowsky, G. Plunien, and D. A. Solovyev, Phys. Rep. **455**, 135 (2008).

[21] O. Yu. Andreev, L. N. Labzowsky, and G. Plunien, Phys. Rev. A **79**, 032515 (2009).

[22] W. R. Johnson, S. A. Blundell, and J. Sapirstein, Phys. Rev. A **37**, 307 (1988).

[23] V. M. Shabaev, I. I. Tupitsyn, V. A. Yerokhin, G. Plunien, and G. Soff, Phys. Rev. Lett. **93**, 130405 (2004).

[24] V. A. Yerokhin, A. Surzhykov, and A. Müller, Phys. Rev. A **96**, 042505 (2017).

[25] A. I. Akhiezer and V. B. Berestetskii, *Quantum Electrodynamics* (Wiley Interscience, New York, 1965).

[26] M. Abramowitz and I. A. Stegun, *Handbook of Mathematical Functions With Formulas, Graphs and Mathematical Tables* (Dover, New York, 1972).

[27] D. A. Varshalovich, A. N. Moskalev, and V. K. Khersonskii, *Quantum Theory of Angular Momentum* (World Scientific, Singapore, 1988).

[28] K. N. Lyashchenko, O. Y. Andreev, and D. Yu, Phys. Rev. A **101**, 040501(R) (2020).